

Alterations in the Cytoskeleton Accompany Aluminum-Induced Growth Inhibition and Morphological Changes in Primary Roots of Maize¹

Elison B. Blancaflor², David L. Jones², and Simon Gilroy*

Biology Department, 208 Mueller Laboratory, The Pennsylvania State University, University Park, Pennsylvania 16802 (E.B.B., S.G.); and School of Agricultural and Forest Sciences, University of Wales, Bangor, Gwynedd, United Kingdom (D.L.J.)

Although Al is one of the major factors limiting crop production, the mechanisms of toxicity remain unknown. The growth inhibition and swelling of roots associated with Al exposure suggest that the cytoskeleton may be a target of Al toxicity. Using indirect immunofluorescence microscopy, microtubules and microfilaments in maize (*Zea mays* L.) roots were visualized and changes in their organization and stability correlated with the symptoms of Al toxicity. Growth studies showed that the site of Al toxicity was associated with the elongation zone. Within this region, Al resulted in a reorganization of microtubules in the inner cortex. However, the orientation of microtubules in the outer cortex and epidermis remained unchanged even after chronic symptoms of toxicity were manifest. Auxin-induced reorientation and cold-induced depolymerization of microtubules in the outer cortex were blocked by Al pretreatment. These results suggest that Al increased the stability of microtubules in these cells. The stabilizing effect of Al in the outer cortex coincided with growth inhibition. Reoriented microfilaments were also observed in Al-treated roots, and Al pretreatment minimized cytochalasin B-induced microfilament fragmentation. These data show that reorganization and stabilization of the cytoskeleton are closely associated with Al toxicity in maize roots.

The trivalent metal Al is solubilized by the low pH of acidic soils and is a major factor limiting crop productivity in many areas of the world. One of the most obvious symptoms of Al toxicity is the rapid inhibition of root growth (Ryan et al., 1993), which results in poor nutrient acquisition and consequently leads to nutrient deficiencies and decreased crop yields (Taylor, 1990; Kochian, 1995). Despite many proposed theories attempting to explain the cause of toxicity, however, the mechanisms involved remain unidentified (Kochian, 1995; Kochian and Jones, 1997).

The cytoskeleton is a dynamic network of proteinaceous components consisting mainly of microtubules and microfilaments. Both of these cytoskeletal components have been

implicated in a wide variety of cellular functions, such as cell division, cell expansion, cell wall synthesis, organelle movement, and tip growth (Seagull, 1989). Compounds that disrupt the normal functioning of the cytoskeleton have been shown to inhibit growth and cause substantial swelling of the root apex, similar to the visual symptoms of Al rhizotoxicity (Baskin et al., 1994; Baluska et al., 1996; Baskin and Wilson, 1997). In addition, several factors that lead to altered growth in roots, such as gravistimulation, osmotic stress (Blancaflor and Hasenstein, 1993, 1995a), and hormone treatments (Baluska et al., 1993a; Blancaflor and Hasenstein 1995b), elicit a reorientation in the microtubule cytoskeleton. Therefore, the growth inhibition and concomitant increase in root diameter observed in roots exposed to Al (Bennet et al., 1985; Ryan et al., 1993; Sasaki et al., 1996) suggest that the plant cytoskeleton could be a cellular target of Al phytotoxicity.

Various neurological disorders induced by Al in experimental animals have also been associated with abnormalities in components of the cytoskeleton (Schmidt et al., 1991; Singer et al., 1997). One proposed model for such cytoskeletal disruption involves Al binding 10⁷-fold more effectively than Mg to the GTP-binding sites on tubulin that are required for microtubule assembly. When Al is associated with the GTP-tubulin complex, the exchange of GTP for GDP is slower. Thus, the intricate dynamics of microtubule formation could be disrupted (MacDonald et al., 1987; MacDonald and Martin, 1988). In addition, the study of Al-induced neurofibrillary tangles in mammalian systems has shown that Al can also affect the expression of cytoskeletal regulatory genes, cytoskeletal protein phosphorylation, and the production of secondary messengers (cAMP, cGMP, inositol 1,4,5-trisphosphate) involved in the regulation of cytoskeletal dynamics (Strong et al., 1997).

Control of plant cytoskeletal organization has been suggested to be under the influence of cellular events and mediated by one or more signal transduction pathways (Cyr and Palevitz, 1995). The phosphoinositide signaling system (Xu et al., 1992; Drobak, 1993) and Ca²⁺/calmodulin (Cyr, 1991; Fisher et al., 1996) have been implicated in the regulation of the plant cytoskeleton and have also been

¹ This work was supported by grants from the National Science Foundation (to S.G.), the North Atlantic Treaty Organization (to D.L.J. and S.G.), the Royal Society, and the Nuffield Foundation (to D.L.J.).

² These authors contributed equally to the paper.

* Corresponding author; e-mail sxg12@email.psu.edu; fax 1-814-865-9131.

Abbreviations: CB, cytochalasin B; FDA, fluorescein diacetate.

proposed as cellular targets of Al toxicity (Siegel and Haug, 1983; Jones and Kochian, 1995, 1997; Jones et al., 1998).

Despite the possibility that the cytoskeleton could be a principal target of Al rhizotoxicity, there have been only a few studies investigating the effects of Al on the plant cytoskeleton. Although it has been shown that Al strongly promotes the polymerization of tubulin subunits into microtubules in vitro (MacDonald et al., 1987; MacDonald and Martin, 1988), microtubules in elongating cells of wheat roots were reported to depolymerize in response to Al (Sasaki et al., 1997). Grabski and Schindler (1995) reported that Al induced a rigidification of the actin network in soybean root suspension cells, and it was recently shown that mRNAs of the actin-bundling protein fimbrin were up-regulated in wheat roots exposed to Al (Ortega et al., 1997). Al has also been shown to inhibit growth in liverwort rhizoids concomitant with a fragmentation of the actin network (Alfano et al., 1993).

The studies cited above clearly indicate that Al could potentially affect the plant cytoskeleton; however, these experiments do not provide a consistent account of this effect. Thus, it is still uncertain whether Al acts by stabilizing, depolymerizing, or causing a reorganization in the cytoskeleton. Furthermore, the link between changes in the cytoskeleton and Al toxicity symptoms in intact roots remains unproved. Therefore, we investigated the effects of Al on the microtubules and microfilaments in elongating cells of maize roots and correlated them with Al-induced growth inhibition. We present data showing that microtubules and microfilaments are altered in both stability and organization when exposed to Al. The data show that Al interactions with cytoskeletal components may be an important factor in Al rhizotoxicity.

MATERIALS AND METHODS

Plant Material

Seeds of maize (*Zea mays* L. cv Merit, Asgrow Seed Co., Kalamazoo, MI) were soaked in distilled water for 10 h and germinated between wet paper towels. Seedlings were grown vertically for 2 d under fluorescent lamps providing continuous diffuse light ($36 \mu\text{mol m}^{-2} \text{s}^{-1}$). Seedlings with straight roots approximately 2 cm in length were selected and transferred to 350-mL clear, plastic chambers containing aerated $200 \mu\text{M}$ CaCl_2 , pH 4.5. Roots were grown hydroponically at 25°C in this solution for 24 h before experimentation.

Growth Measurements and Al Treatments

Straight roots, approximately 3 to 4 cm in length, were selected and marked with black oil-based Speedball ink at 1-mm intervals from the root tip. One-half of the marked roots were returned to the solution containing $200 \mu\text{M}$ CaCl_2 , pH 4.5 (controls), and the other half were placed in a solution containing $200 \mu\text{M}$ CaCl_2 , $50 \mu\text{M}$ AlCl_3 , pH 4.5 (Al^{3+} activity = $27.8 \mu\text{M}$ assuming no $\text{Al}(\text{OH})_3$ precipitation). The length of each segment was measured from

digitized images of the marked roots 2 h after treatment. In another set of growth measurements, elongation of the whole root was measured for 12 h at 20-min intervals. For root-diameter changes, images of roots were captured every 2 h for 10 h. Root diameter was measured at 1-mm intervals along the length of the root, with the tip of the cap designated as 0. Images of roots were collected at each time point using a 100-mm Promaster Macro lens (Nikon) attached to a video camera (model C2400, Hamamatsu, Tokyo, Japan) and captured with a LG-3 frame grabber (Scion Corp., Frederick, MD) and Quadra 800 computer (Apple Computer Inc., Cupertino, CA) running IPLabs Spectrum image-acquisition software (Signal Analytics, Vienna, VA).

Light Microscopy of Roots

Plants were grown hydroponically as described above and treated with or without Al ($50 \mu\text{M}$) for 24 h. The terminal 7 mm of the roots was then excised and fixed under a partial vacuum in 3% (w/v) glutaraldehyde, 50 mM sodium phosphate buffer, pH 7.2, for 24 h. After fixation, tissue samples were dehydrated through an ethanol series (25%, 50%, 75%, and 100% [v/v] ethanol for 12 h each), exchanged with acetone (100%, v/v), exchanged back to ethanol (100%, v/v), and resin embedded using a historesin embedding kit (Leica Instruments, Heidelberg, Germany). Embedded roots were then sectioned ($4 \mu\text{m}$ thick) on a microtome (model 2050, Reichert-Jung, Heidelberg, Germany) using glass and tungsten-carbide steel knives, stained for 2 h in toluidine blue (0.05% [w/v] in benzoate buffer, pH 4.0), and visualized using a LSM410 confocal microscope (Zeiss).

Assessment of Cell Viability

To confirm the viability of root cells, plants were exposed to Al ($50 \mu\text{M}$) for 24 h as described above and then stained with FDA (0.05% [w/v]; Sigma) for 5 min as described by Huang et al. (1986). After washing (1 min), the fluorescence of cells within the elongation zone of control and Al-treated roots was then imaged with a confocal microscope, with excitation at 488 nm and emission at 515 to 540 nm.

Immunofluorescence

Indirect immunofluorescent labeling of microtubules and microfilaments was essentially performed as described by Blancaflor and Hasenstein (1993, 1997) with minor modifications. After the experimental treatments, the terminal 7 mm of the roots was excised and placed into glass vials containing fixative. For preserving microtubules the fixative consisted of PHEMD buffer (60 mM Pipes, 25 mM Hepes, 10 mM EGTA, 2 mM MgCl_2 , and 5% [v/v] DMSO), pH 7.0, plus 4% (w/v) formaldehyde (Blancaflor and Hasenstein, 1993), whereas fixative for preserving microfilaments consisted of 2% formaldehyde in PHEMD buffer,

pH 7.0 (Blancaflor and Hasenstein 1997). After 2 h in fixative, roots were washed (3×5 min each) in PHEMD buffer, attached to a metal block with cyanoacrylate (Krazy Glue, Borden Inc., Columbus, OH), and sectioned longitudinally with a Vibratome-1000 (Technical Products International, St. Louis, MO) at a thickness of $80 \mu\text{m}$. Median longitudinal sections were transferred to glass slides coated with poly-L-Lys (Sigma) and allowed to dry for 5 min. Sections were partially digested for 10 min in an enzyme solution consisting of 1% (w/v) cellulase (Yakult, Tokyo, Japan), 0.01% (w/v) pectolyase (Sigma), and 1% (w/v) BSA followed by 15 min of incubation in 1% (v/v) Triton X-100. Sections were then incubated in the primary antibodies for 2 h.

For labeling microtubules, sections were incubated in rat anti-yeast tubulin (clone YOL 1/34, Accurate Chemical and Scientific Corp., Westbury, NY). For labeling actin, a mouse monoclonal antibody to phalloidin-stabilized pea actin was used (Andersland et al., 1994). Sections were then incubated in the dark with the appropriate secondary antibodies conjugated to fluorescein isothiocyanate (goat anti-rat IgG for microtubules and rabbit anti-mouse IgG for microfilaments; Sigma). After three washes in PHEMD buffer, sections were mounted in 20% Mowiol 4-88 (Calbiochem, La Jolla, CA) in PBS, pH 8.5, containing 0.1% *p*-phenylenediamine (Sigma). Cytoskeletal elements were imaged with a confocal microscope, with excitation at 488 nm and emission at 515 to 540 nm. Images from the confocal microscope were assembled using Photoshop 3.0 (Adobe Systems, Inc., Mountain View, CA) and printed on a dye-sublimation printer (Phaser II SDX, Tektronix, Inc., Wilsonville, OR).

Auxin, Cold, Taxol, and CB Treatment

A stock solution of 10 mM IAA (Sigma) was prepared in 2-propanol. CB (Calbiochem) was prepared as 10 mM stock solutions in 100% DMSO. The required volumes of IAA and CB stock were added to separate sets of roots growing in $200 \mu\text{M}$ CaCl_2 , pH 4.5, with or without $50 \mu\text{M}$ Al. The final concentration of IAA in the solution was $1 \mu\text{M}$, and for CB, $50 \mu\text{M}$. IAA-treated roots were fixed and processed for microscopy after 1 h of incubation, whereas CB-treated roots were processed after 3 h. For cold treatment, a solution containing $50 \mu\text{M}$ Al was prechilled to 2°C . Roots grown at 25°C for up to 12 h in solutions containing Al were transferred to 2°C solutions for 2 h and processed for microscopy.

For taxol experiments, a stock of 20 mM taxol (Fluka) was prepared in 100% DMSO. A working solution of $20 \mu\text{M}$ taxol was made by adding the required volume of the stock solution to $200 \mu\text{M}$ CaCl_2 , pH 4.5. Roots were fixed after 12 and 48 h of incubation in taxol and processed for microscopy. In another set of experiments roots were incubated in taxol solution for 3 h, transferred to a solution containing $1 \mu\text{M}$ IAA for 1 h, and processed for microscopy. Solvent controls (0.5% [v/v] DMSO or 0.01% [v/v] propanol) showed no effect on growth or cytoskeletal organization.

RESULTS

Effects of Al on Growth, Morphology, and Viability of Maize Root Cells

Growth rates of maize roots were inhibited by Al in a concentration-dependent manner. Less than 20% inhibition occurred at $5 \mu\text{M}$, and greater than 60% inhibition occurred at concentrations at or above $50 \mu\text{M}$ (Fig. 1A). Because maximum root-growth inhibition under our conditions occurred at Al concentrations of $50 \mu\text{M}$ or greater (Fig. 1A), all subsequent experiments were performed on roots grown hydroponically in the presence or absence of $50 \mu\text{M}$ Al. The growth of maize primary roots proceeded at a rate of approximately 1.5 mm h^{-1} under control conditions. Application of $50 \mu\text{M}$ Al resulted in a rapid decline in the growth rate, consistent with results presented previously for Al-sensitive varieties of wheat (Jones and Kochian, 1995) and maize (Sivaguru and Horst, 1998). The root-growth rate was reduced by 50% after 2 h and by 80% after 12 h (Fig. 1B), with a complete inhibition of growth evident after 24 h of Al exposure (data not shown).

Growth inhibition after Al exposure was most pronounced in the region 2 to 5 mm from the root tip after 2 h (Fig. 1C). This pattern was maintained for as long as we monitored the roots (6 h; data not shown) and was similar to the inhibitory effect of Al reported for squash roots (Le Van et al., 1994). For this reason, all later studies concentrated on the zone of elongation 2 to 5 mm from the root cap. In addition to the rapid inhibition of root growth, Al also induced an increase in root diameter over longer periods (>4 h); however, this appeared to be limited to distances from 3 to 5 mm from the root cap (Fig. 1D). Prolonged exposure to Al (>12 h) also resulted in severe morphological distortions in the root-elongation zone, as shown by swollen cells within the inner cortex and large holes in the root surface produced by the loss of both epidermal and outer cortical groups of cells (Fig. 2, A and B; see also Fig. 6). Despite an obvious degeneration of the root cortex, studies with the vital stain FDA showed no loss of cell viability in control or Al-treated cells in the cortical and epidermal regions, indicating that Al does not act as a generic cytotoxin (Fig. 2, C and D).

Effect of Al on Microtubule Organization

The organization of microtubules in primary roots of maize exposed to $50 \mu\text{M}$ Al for various periods (1–24 h) was examined by indirect immunofluorescence microscopy. In control roots cortical microtubules in the elongation zone were oriented perpendicular to the long axis of the root in the outer cortex (Fig. 3A), inner cortex (Fig. 3B), and stele (Fig. 3C). This pattern of microtubule orientation was observed throughout the apical 6 mm of the root. At 6 to 7 mm from the root tip, cortical microtubules shifted to an oblique orientation typical of all cell layers in the maturation zone (Fig. 3D). These results are consistent with those of previous studies (Blancaflor and Hasenstein, 1993, 1995b).

Upon initial exposure to Al (1–2 h), the organization of microtubules in the elongation zone (2–5 mm from the root

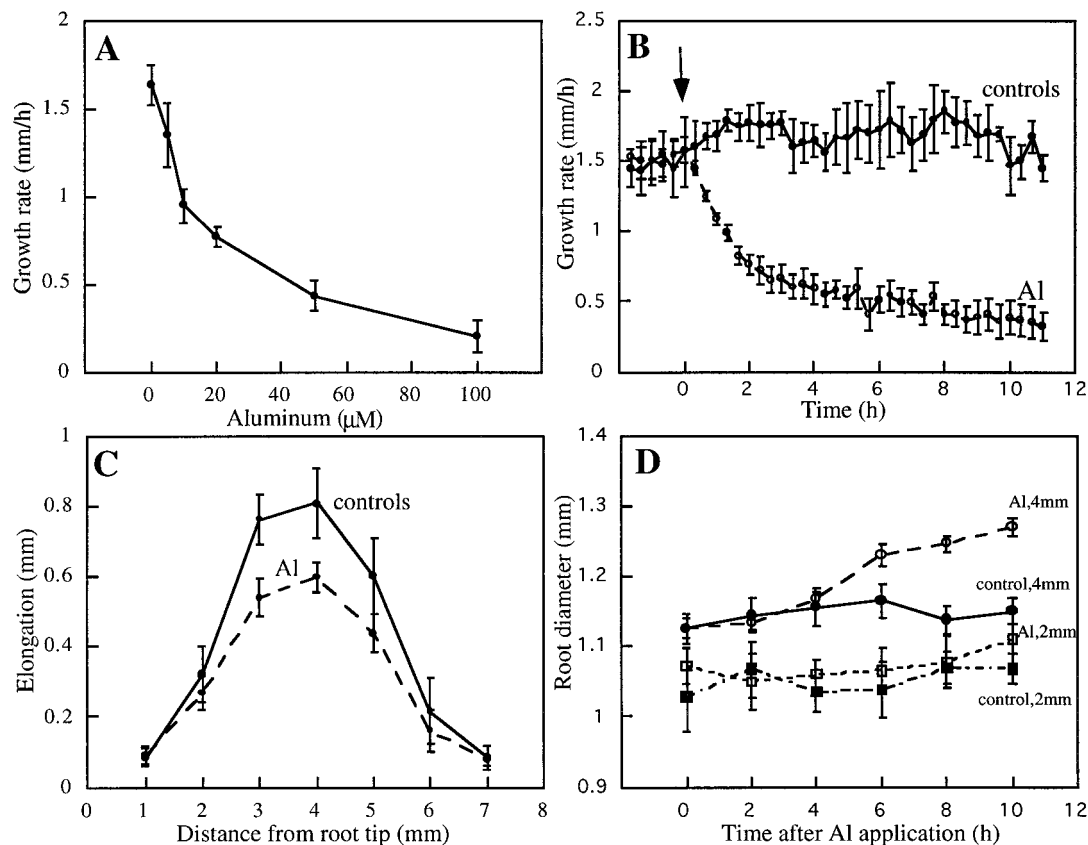


Figure 1. Effects of Al on elongation and radial expansion of maize roots. A, Dose-response curve of root-growth inhibition by Al. Seedlings were transferred to aerated solutions containing the indicated concentrations of Al and the root growth was measured after 6 h. Concentrations at or above 50 μM Al resulted in maximum growth inhibition. B, Kinetics of axial root-growth rate of untreated roots (control) and roots in response to 50 μM Al. The growth rate of roots declined within 1 h of Al application (arrow). C, Effect of 50 μM Al on elongation growth within different regions of the root. Roots were marked at 1-mm intervals from the tip, and extension of the marked segments was measured 2 h after exposure to Al. Growth of the region 2 to 5 mm from the root tip was the most effectively inhibited by Al. D, Kinetics of radial expansion at 2 and 4 mm from the tip of maize primary roots treated with 50 μM Al. Swelling was perceptible more than 3 mm from the tip 6 h after Al exposure. No swelling was observed less than 2 mm from the tip during the initial 10 h of Al treatment. Data points are means from six or more roots \pm SE.

cap) did not differ from that in control roots (data not shown); however, after 3 h of Al exposure, cells in the three layers of the inner cortex 4 to 5 mm from the root cap had started to display microtubules oriented in either a random or an oblique pattern (Fig. 4A). This zone of reorientation moved progressively closer to the root apex upon prolonged exposure to Al, with microtubules in the inner cortex of the entire elongation zone becoming reoriented by 12 h (Fig. 4B). After 4 to 5 h of Al exposure, the pattern of microtubules in the stele had also changed from their typically ordered and transverse orientation to being primarily longitudinal (compare Figs. 3C and 4C). Despite the reorganization of microtubules in the inner cortex and stele, the orientation of microtubules in cells of the outer cortex and epidermis remained principally transversely oriented after 4 h (Fig. 4D) and even after prolonged exposure (>12 h; Fig. 4E). Although microtubules of inner cortical cells in the elongation zone were clearly reorganized after Al treatment, microtubules of all cell layers in the maturation zone

did not appear to be affected by Al and remained similar to those of control roots (compare Figs. 3D and 4F).

Al Prevents Auxin-Induced Microtubule Reorientation and Cold-Induced Microtubule Depolymerization

In addition to affecting the organization of microtubules within cells, Al may also be able to affect the stability of cytoskeletal elements either directly or indirectly. This is supported by *in vitro* studies in which Al has been shown to promote tubulin assembly into microtubules (MacDonald et al., 1987). To determine whether the stability of microtubules is affected by Al, we exposed roots to agents known to reorient or depolymerize microtubules either before or after pretreatment with Al.

Auxin has been shown to cause microtubules in cortical cells of maize roots to reorient from a primarily transverse to a longitudinal pattern (Blancaflor and Hasenstein, 1995b), and has also been reported to induce the depoly-

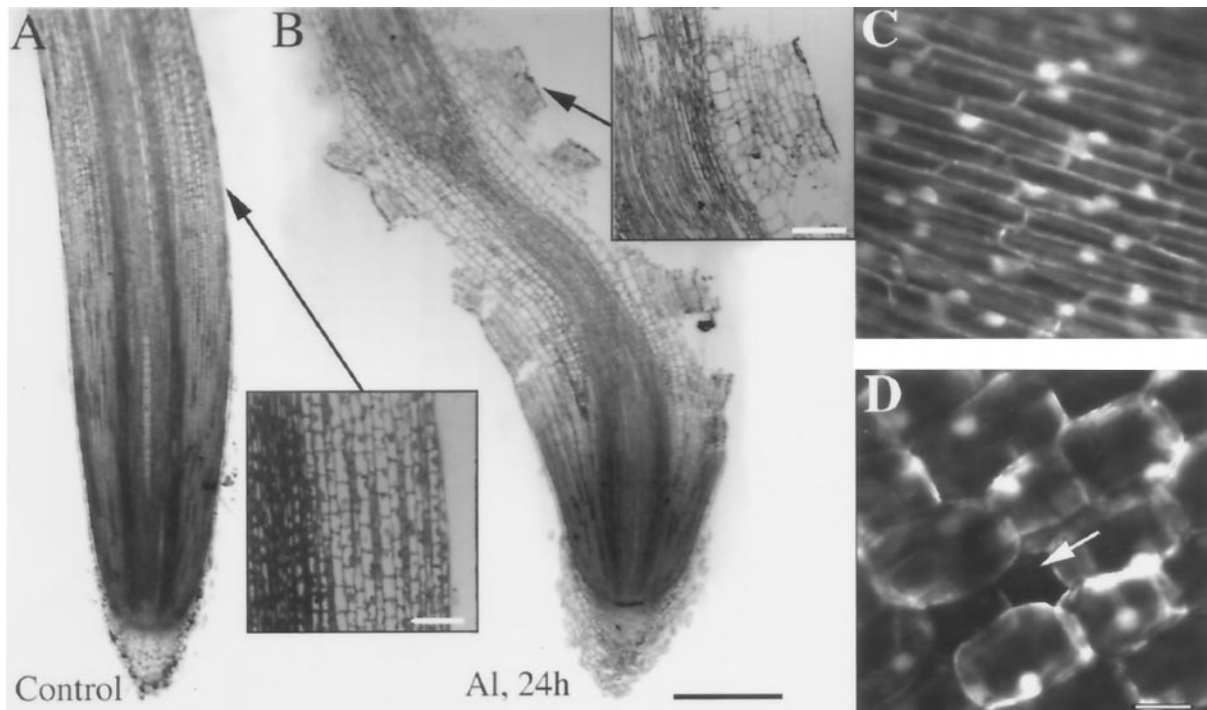


Figure 2. Light micrographs and viability staining of maize primary roots after exposure to $50 \mu\text{M}$ Al. Roots were fixed and embedded in historesin, and a median longitudinal section was taken from control roots (A) and roots 24 h after Al treatment (B). Inset in A shows a magnified view of the surface of an untreated root. Inset in B shows a magnified view of the surface lesions of an Al-treated root. These lesions were not generated by a sectioning artifact, as shown in Figure 6. Confocal sections of the fluorescence from cells at the surface of control (C) and Al-treated (D) roots stained with the viability stain FDA show that despite the degeneration of the root cortex and holes (arrow) in the surface layer of cells, the cells at the surface of the Al-treated root are viable. Images are representative of at least 50 independent root samples. Bar in B = 1 mm; bars in insets = $100 \mu\text{m}$; and bar in D = $25 \mu\text{m}$ and applies to C and D.

merization of microtubules (Baluska et al., 1996). To test the possibility that Al may be altering either the stability or the ordering of microtubules, roots were incubated with or without Al before treatment with auxin.

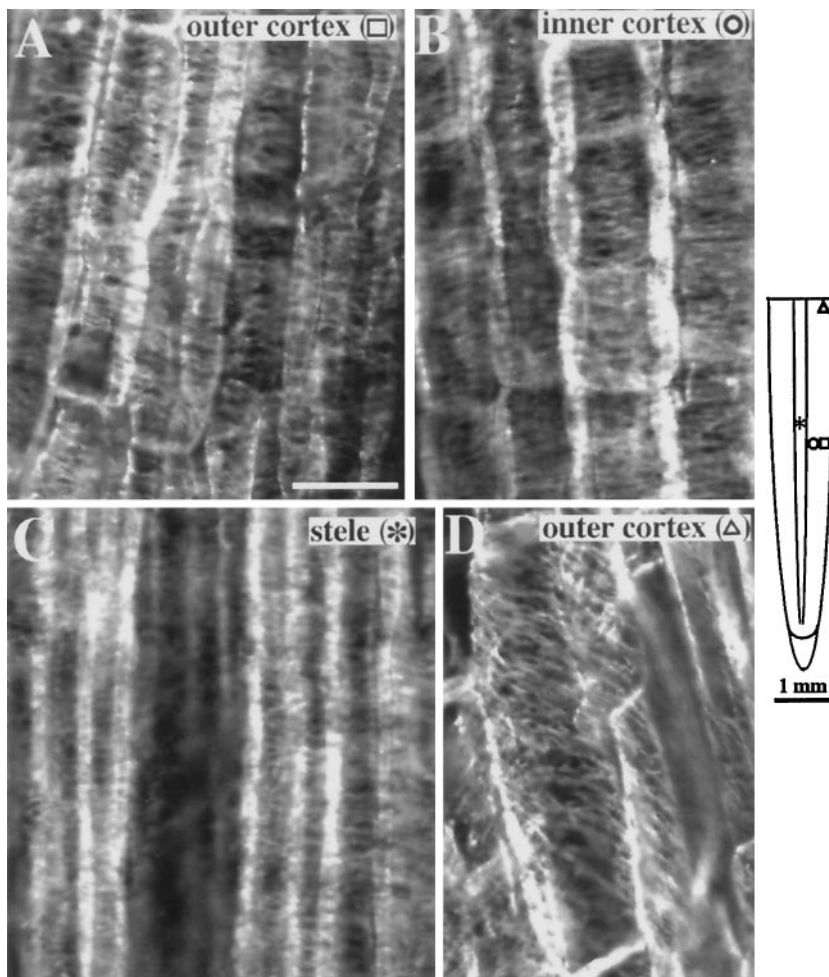
Roots grown in the absence of Al followed by a 1-h exposure to $1 \mu\text{M}$ IAA displayed a characteristic reorientation of microtubules from transverse to longitudinal arrays in both the outer (Fig. 5A) and inner cortex (data not shown) of the elongation zone, in agreement with Blancaflor and Hasenstein (1995b). In contrast, roots incubated in $50 \mu\text{M}$ Al for 1 h before IAA application did not show an IAA-induced reorientation of the microtubules in the outer cortex (Fig. 5B), but did show the reorientation of microtubules in the inner cortex to principally longitudinal arrays (data not shown).

Another treatment known to depolymerize microtubules in roots is cold temperatures (Baluska et al., 1993b). Microtubules of roots incubated at 2°C for 2 h were extensively fragmented (Fig. 5C). Roots pretreated for 3 h with Al before cold application had a greater density of intact microtubules (Fig. 5D). This effect was representative of up to 12 h of Al pretreatment. Only 39% of cells in the outer cortex of roots exposed to cold had intact microtubules. However, in roots pretreated with Al before cold application, 87% of outer cortical cells had intact microtubules (Fig. 5E).

To further test the interaction between Al and cytoskeletal elements, we compared the organization of microtubule arrays after treatment with taxol, a drug known to promote microtubule assembly and stabilize preexisting microtubules in plant cells (Bokros et al., 1993; Chu et al., 1993), with those of Al-treated roots. Our rationale for doing this was based on observations showing that the morphology of roots exposed to Al was visually similar to that of roots treated with taxol. Taxol-treated roots exhibited a distinct swelling along the elongation zone and eventually developed lesions along the surface of the root, similar to those seen under Al toxicity. However, these symptoms took longer (i.e. >48 h) to develop than was observed for Al (24 h; Fig. 6).

Examination of microtubules in the outer cortex of 12-h taxol-treated roots revealed bundled, dense, and highly ordered microtubule arrays (Fig. 7A). Although 12 h of Al exposure did not result in increased ordering of microtubules, bundling was more extensive compared with controls, as shown by the increased lateral association between microtubules (Fig. 7B). Control roots exhibited bundled microtubules, but the degree of bundling was lower (Fig. 7C; see also Fig. 1). After 48 h, the cells in the cortex of taxol-treated roots were no longer elongated but displayed distorted shapes similar to those of Al-treated roots. Despite the distorted appearance of these cells, an overall

Figure 3. Organization of cortical microtubules in maize primary roots grown in $200 \mu\text{M}$ CaCl_2 , pH 4.5 (controls). Along the elongation zone (approximately 2–5 mm from the root tip), the outer (A) and inner (B) cortex of control roots show microtubules aligned perpendicular to the long axis of the root. C, Stele cells in the same region also show transverse microtubules. D, Microtubules shift to an oblique orientation 6 to 7 mm from the root tip. The schematic diagram of the root indicates the regions where immunofluorescence images were obtained. Symbols in parentheses in A to D correspond to the symbols in the root diagram. Images are representative of at least five independently processed root samples. Bar in A = $25 \mu\text{m}$.



transverse alignment of microtubules was still apparent in both the outer (Fig. 7D) and inner cortex (data not shown). Microtubules in outer cortical cells of 24-h Al-treated roots also retained an overall transverse microtubule alignment with extensive bundling (Fig. 7E). Roots treated with $20 \mu\text{M}$ taxol for 3 h followed by 1 h in $1 \mu\text{M}$ IAA exhibited transverse microtubules in the outer cortex (Fig. 7F).

Effects of Al on Microfilament Organization

Cells in the elongation zone of untreated control roots showed microfilaments predominantly longitudinal in orientation present in both the outer and inner cortex, as well as in the stele parenchyma (Fig. 8, A–C). There were no gross qualitative changes in the organization of microfilaments treated with Al during the initial 5 h of exposure (data not shown). However, greater than 6 h of Al exposure resulted in microfilaments in the inner cortex becoming more random in orientation (Fig. 8D). In contrast, microfilaments in the outer cortical cells remained longitudinal in orientation and similar to controls (Fig. 8E). Disruption of the actin network in the inner cortex was severe after 8 to 24 h of Al treatment. Thick actin cables were randomly oriented and appeared to radiate from the nucleus (Fig. 8F); however, finer strands of randomly oriented actin

bundles were also present throughout the cell (Fig. 8G). Outer cortical cells after 24 h of exposure to Al also showed thicker microfilament cables but the predominant alignment was still in the longitudinal direction, as in non-treated cells (Fig. 8H). Despite a disruption of microfilament organization in cells of the inner cortex within 6 to 24 h of Al exposure, microfilaments in the stele parenchyma cells remained longitudinal. However, the microfilament bundles in these cells appeared thicker than those in controls (Fig. 8I).

To test whether Al can induce a stabilization of microfilaments in intact maize tissues, roots were pretreated with Al before application of the known actin-depolymerizing compound CB. Exposure of roots to $50 \mu\text{M}$ CB for 3 h resulted in an extensive fragmentation of the actin network in cortical cells throughout the elongation zone (Fig. 9A), with some lesser fragmentation evident in the stele. Remaining microfilament bundles were also thinner and less dense in the stele of CB-treated roots compared with controls (Fig. 9B). These results are consistent with those of a previous study (Blancaflor and Hasenstein, 1997). Roots pretreated with Al for 3 to 12 h before CB application also exhibited some limited fragmentation of the actin network; however, many cells in both the inner and outer cortex retained a high density of thick microfilament cables (Fig.

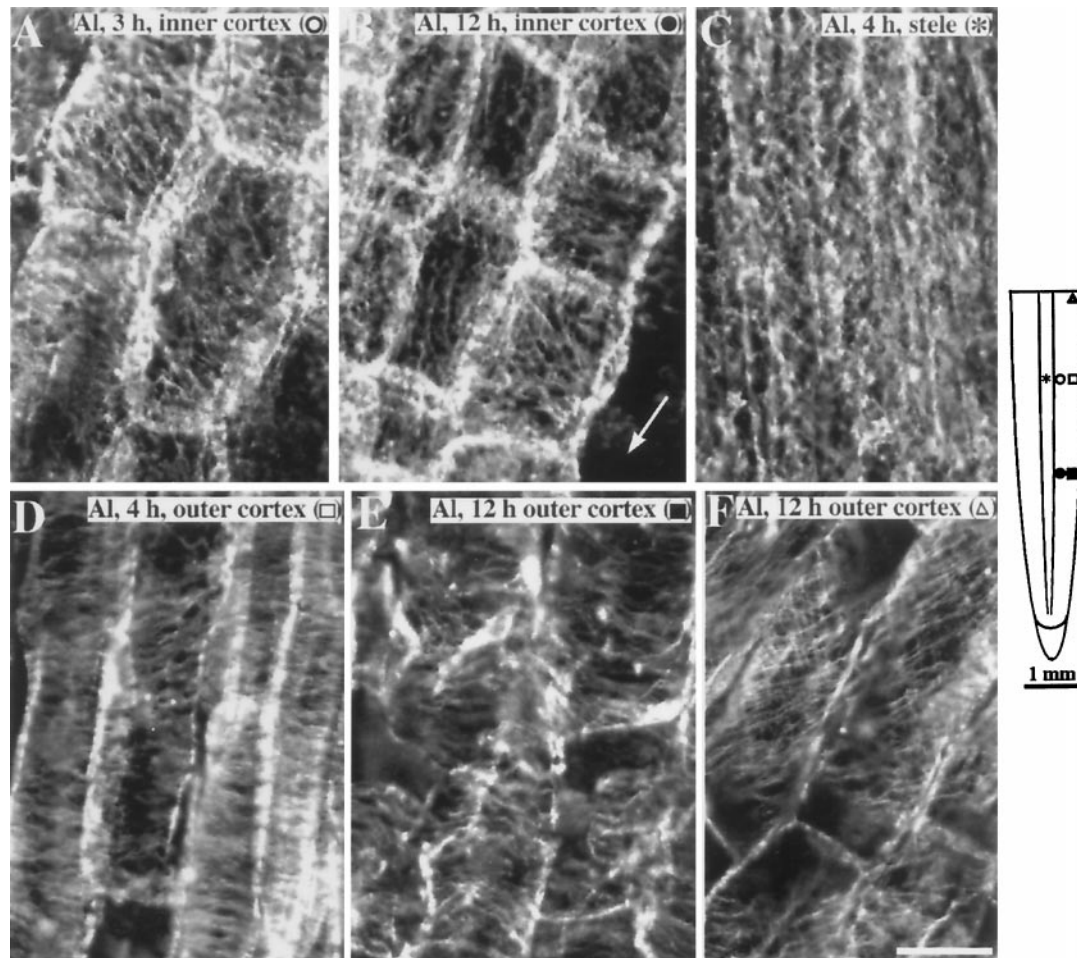


Figure 4. Organization of cortical microtubules in maize primary roots after exposure to 50 μM Al. A, After 3 h of continuous exposure to Al, cells in the inner cortex 4 to 4.5 mm from the root tip showed random and obliquely oriented microtubules. B, After 12 h of continuous exposure to Al, reoriented microtubules occurred closer to the root tip. Cells in the inner cortex 2 mm from the tip showed random to longitudinally oriented microtubules. Arrow shows region where outer cortex has sloughed off. C, The stele cells also exhibited random to longitudinal microtubules but occurred after 4 h of Al exposure. D, Four hours after Al exposure, outer cortical cells 4 mm from the root tip retained their net transverse microtubule orientation. E, Outer cortical cells 12 h after Al exposure also retained an overall transverse alignment of microtubules despite the distorted appearance of the cells. F, Cells in the maturation zone (about 6 mm from the tip) showed oblique microtubules that were similar to controls. The schematic diagram of the root indicates the regions where immunofluorescence images were obtained. Symbols in parentheses in A to F correspond to the symbols in the root diagram. Images are representative of at least five roots per time point. Bar in F = 25 μm .

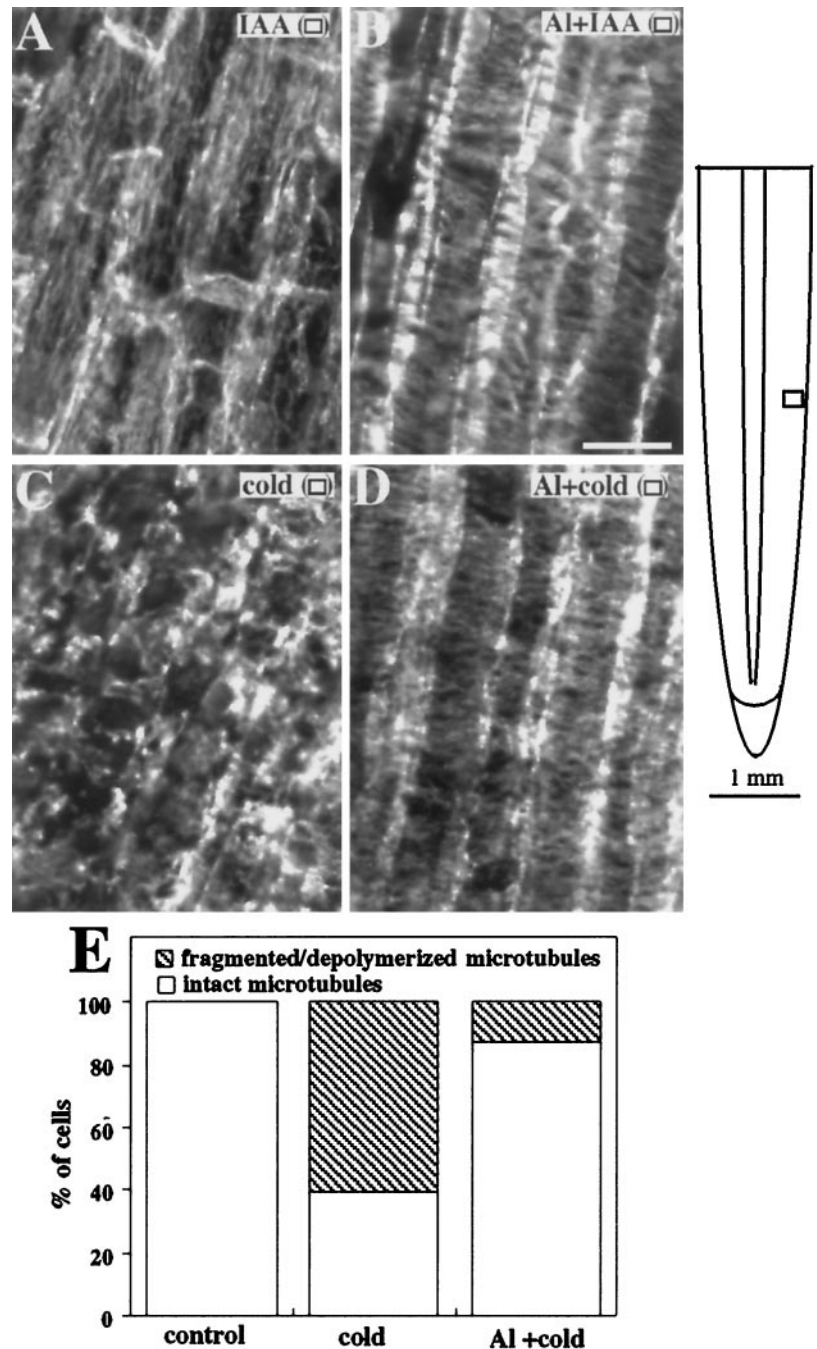
9C). Microfilaments in the stele were also more resistant to the effects of CB. Microfilament bundles remained dense and thicker than in roots not treated with Al (Fig. 9D). In roots treated with CB only 15% of cells in the outer cortex had an intact array of microfilaments. Incubation in Al for 3 h before CB application resulted in a higher percentage (68%) of cells in the outer cortex with thick bundles of microfilaments (Fig. 9E).

DISCUSSION

Despite the advancement of many theories to explain the cause of Al toxicity in plants, the initial target sites still remain unknown (Kochian, 1995; Kochian and Jones, 1997). It has recently been hypothesized from experiments with

cell-suspension cultures that one of the primary mechanisms of Al toxicity in plants may be associated with an increased rigidity of the actin network (Grabski and Schindler, 1995). In addition, Al has also been shown to promote the assembly of microtubules *in vitro* (MacDonald et al., 1987). However, there are also conflicting reports suggesting that Al toxicity operates by causing a depolymerization of both microtubules and microfilaments (Alfano et al., 1993; Sasaki et al., 1997). Although these studies are consistent with the hypothesis that the cytoskeleton could be a potential Al target site, a correlation of the observed changes with those of the temporal dynamics of growth inhibition has yet to be reported. Thus, an assessment of whether the cytoskeleton is an initial symptom or a more indirect or secondary symptom of Al exposure has not been

Figure 5. Organization of cortical microtubules in maize primary roots treated with IAA, Al, or cold. A, Microtubules in cells of the outer cortex shifted to longitudinal orientations after 1 h of exposure to $1 \mu\text{M}$ IAA. B, Microtubules in cells of the outer cortex exposed for 1 h to $50 \mu\text{M}$ Al followed by 1 h in $1 \mu\text{M}$ IAA remained transversely oriented. C, Roots incubated in 2°C solution for 2 h showed fragmented microtubules. D, Roots pretreated with Al for 12 h before cold exposure still had cells with intact microtubules. E, The fraction of cells in the outer cortex of cold-treated and Al-plus-cold-treated roots were classified by whether they had intact or fragmented/depolymerized microtubules. At least 50 cells were observed for each treatment. Images are representative of at least three roots from three independent experiments. The schematic diagram of the root indicates the regions where immunofluorescence images were obtained. Symbols in parentheses in A to D correspond to the symbols in the root diagram. Bar in B = $25 \mu\text{m}$.



possible. Therefore, we conducted a detailed immunofluorescence study on the effect of Al on the organization of microtubules and microfilaments in maize roots and correlated these effects with growth inhibition and radial expansion of roots.

The data presented here indicate that toxic levels of Al result in a significant cell-specific reorganization and stabilization of the root's cytoskeleton, as summarized in Figure 10. The effect of Al on the reorganization of the cytoskeleton was evident in the root-elongation zone, consistent with results showing that this root zone is where Al toxicity is first detectable (Ryan et al., 1993; Sivaguru and

Horst, 1998). Generally, the effect of Al on the cytoskeleton was rapid, coincided with the time course of growth inhibition, and was more pronounced for microtubules than for microfilaments. In contrast to a previous study showing that Al induced a depolymerization of cortical microtubules in wheat roots (Sasaki et al., 1997), experiments performed here with maize demonstrated that Al can induce a significant stabilization of microtubules even in cells showing chronic symptoms of Al stress.

Al toxicity is commonly associated with a swelling of the root apex (Bennet et al., 1985; Ryan et al., 1993). Under the conditions used here, radial expansion of the roots was first

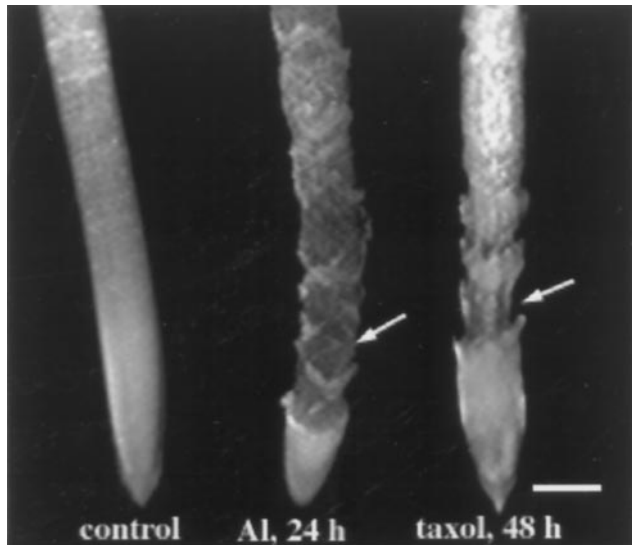


Figure 6. Morphology of maize primary roots after exposure to 50 μM Al or 20 μM taxol. Like Al-treated roots, taxol-treated roots showed disintegration of outer cell layers (arrows) compared with untreated roots (control). By 24 h swelling was no longer apparent because portions of the epidermis and outer cortex had sloughed off. Bar = 1 mm.

detected 6 h after Al exposure and appeared to be caused by the abnormal isodiametric expansion of cells located within the inner cortex (Fig. 2B). Our observation of a selective, Al-induced microtubule reorientation in these inner cortical cells, coupled with the widely proposed model for microtubule orientation controlling cell expansion (Giddings and Staehelin, 1991), may provide a mechanism to explain the Al-induced inner cortical cell expansion leading to root swelling. However, it still remains unclear from our studies whether the observed reorientation of microtubules in the inner cortex is a direct effect of Al or occurs in response to some secondary effector triggered by Al stress.

Growth inhibition was detectable within 1 h (Fig. 1) and obvious reorientation of microtubules in the inner cortex was detected after 3 h. Although Al can penetrate the outer two to three layers of the root within 30 min (Lazof et al., 1994), most of it remains concentrated in the epidermal and outer cortical cells even after a 24-h exposure (Delhaize et al., 1993). Therefore, it is likely that the disruption of microtubules in the inner cells could be an indirect effect of Al. It is interesting to note that tissue-specific disruption of microtubules in the inner cortex of maize roots has also been reported to occur in ethylene-treated roots (Baluska et al., 1993a). Studies on the relationship between Al toxicity and stress-related ethylene synthesis (Reid, 1995) may provide important insight into the mechanism of Al-induced microtubule reorientation and defense responses (e.g. callose production) in inner cortical cells.

In contrast to the inner cortex, the overall orientation of microtubules in the outer cortex and epidermis did not change upon Al exposure. However, the microtubules in these tissues became increasingly stabilized and resistant to depolymerization after Al application. This is similar to

in vitro reports in mammalian systems demonstrating that Al binding to microtubules and neurofilaments can significantly delay their depolymerization (MacDonald et al., 1987; MacDonald and Martin, 1988; Nixon et al., 1990; Shea et al., 1992). The stabilizing effect of Al on the microtubules of cells on the outer cortex was demonstrated by our auxin experiments, which showed that even 1 h of Al exposure could block the IAA-induced reorientation of microtubules from transverse to longitudinal arrays. Although the data presented here cannot resolve the mechanisms by which Al prevented auxin-induced microtubule reorientation, the stabilization caused by Al was rapid (<1 h) and thus coincides with the inhibition of root growth. The stabilizing effect of Al on the microtubules of the outer cortex was also supported by other indirect observations, including: (a) microtubules in Al-treated roots were less susceptible to cold-induced microtubule depolymerization; (b) an increase in bundling frequency in the microtubules of the outer cortex for both taxol and Al-treated roots; and (c); taxol, like Al, prevented auxin-induced microtubule reorientation.

The hypothesis that this stabilization of the microtubule network may be partially responsible for inhibition of root growth is supported by the very similar morphology of Al-treated roots with that of roots treated with the microtubule-stabilizing drug taxol (see Fig. 6). Furthermore, stabilizing microtubules in the transverse orientation with taxol has also been shown to inhibit elongation growth (Baluska et al., 1997; Weerdenburg and Seagull, 1988; this study). Therefore, in addition to the orientation of microtubules (Giddings and Staehelin, 1991), it has been suggested that a dynamic microtubule network could also play an important role in the control of elongation growth (Weerdenburg and Seagull, 1988; Baskin et al., 1994).

Although taxol- and Al-treated roots exhibited similar morphology, there were distinct differences in the onset of these effects. Radial expansion in Al-treated roots was detected after 6 h, whereas for taxol-treated roots expansion was detected only after 15 to 20 h. Lesions in the surface of Al-treated roots were observed as early as 12 h after exposure, whereas lesions in taxol-treated roots were observed only after 48 h (Fig. 6). Furthermore, microtubules in the inner cortex of taxol-treated roots did not reorient but were stabilized in the transverse orientation. These differences suggest that a taxol-like stabilization of the microtubule network by Al may not be singly responsible for the inhibition of root growth. In addition to the effect of Al on the stability of microtubules in the outer cortex, other growth-dependent processes that are independent of microtubules may be simultaneously altered by Al exposure and thus could account for the more pronounced and rapid effect of Al on the growth and morphology of maize roots.

The concentration of Al chosen for this study (50 μM) was the lowest that caused the maximal inhibitory effect on root growth rate (Fig. 1A) and the most pronounced effect on subsequent toxicity symptoms, such as swelling and the development of lesions (Figs. 2 and 6). However, concentrations lower than 50 μM also caused some growth inhibition (Fig. 1A) and root swelling (data not shown). Pre-

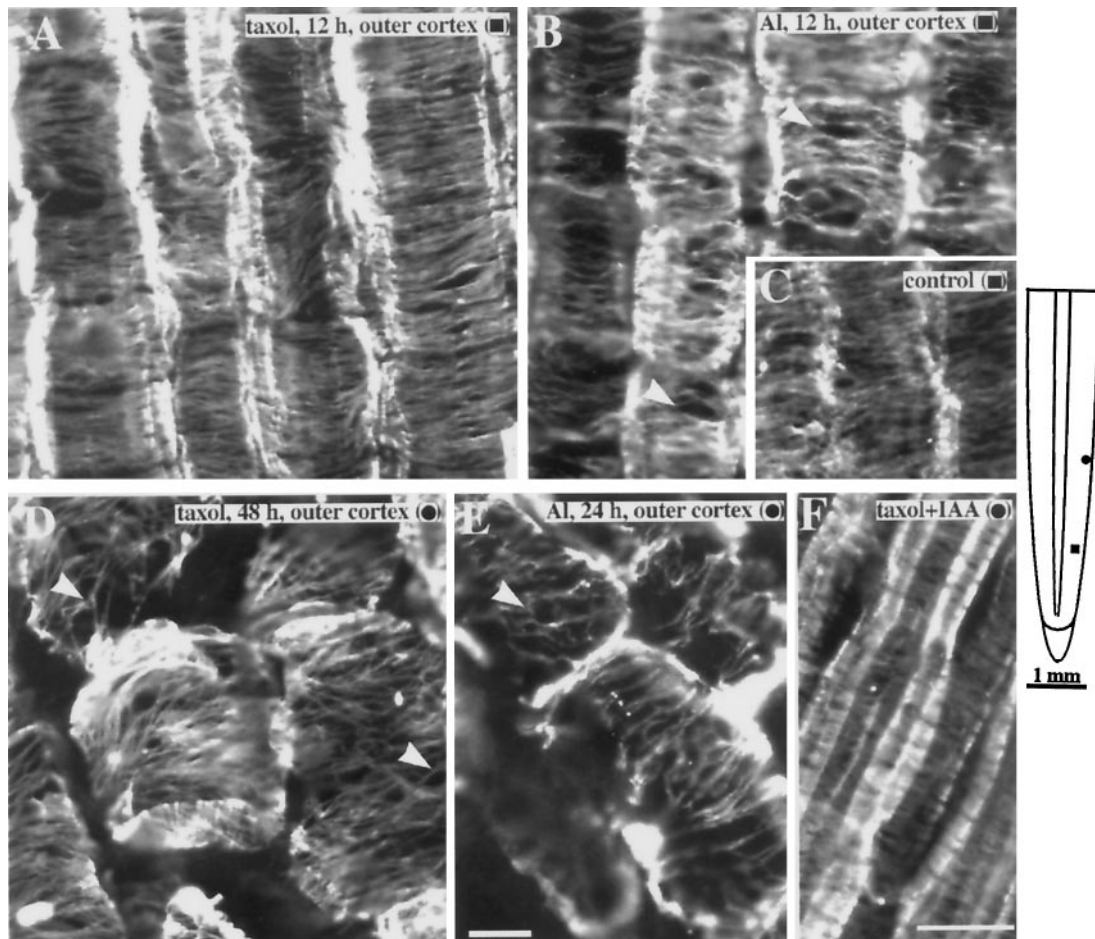


Figure 7. Comparison of cortical microtubule organization in maize primary roots treated with taxol or Al. A, Microtubules in taxol ($20 \mu\text{M}$)-treated roots were higher in density and displayed extensive bundling compared with controls. Bundling was characterized by an increased lateral association of microtubules. B, Although not as dense as microtubules in taxol-treated roots, $50 \mu\text{M}$ Al caused the formation of bundled microtubules (arrowheads). For comparison, the low degree of bundling in untreated controls is shown in C. D, Outer cortical cells after 48 to 60 h of exposure to $20 \mu\text{M}$ taxol showed an overall transverse alignment of microtubules despite distorted cell shapes. E, Region where the outer cortical cells in the elongation zone remained intact even after 24 h of exposure to $50 \mu\text{M}$ Al. Like taxol-treated roots, microtubules retained an overall transverse alignment and displayed extensive bundling (arrowhead). F, Cortical microtubules of roots incubated in taxol for 3 h followed by 1 h of incubation in $1 \mu\text{M}$ IAA remained dense and transversely oriented. Images are representative of at least five roots per treatment. The schematic diagram of the root indicates the regions where immunofluorescence images were obtained. Symbols in parentheses in A to F correspond to the symbols in the root diagram. Bar in E = $10 \mu\text{m}$ and applies to A to E; bar in F = $25 \mu\text{m}$.

liminary results showed that 12 h of exposure to 10 and $20 \mu\text{M}$ Al caused reorientation of microtubules in the inner cortex (E.B. Blancaflor, D.L. Jones, and S. Gilroy, unpublished data). However, it is not known from this study whether the lower concentrations of Al result in microtubule reorientation within the same time frame as $50 \mu\text{M}$ Al or if at these lower Al concentrations microtubules in the outer cortex are still stabilized. Having established the patterns of cytoskeletal effects of an Al concentration causing maximum effects on growth rate, it will be important to determine the threshold Al concentration to elicit these effects on the cytoskeleton.

Like microtubules, actin microfilaments were well preserved even after long exposure to Al, but a qualitative assessment of these changes proved more difficult than for

microtubules because of their less-ordered cellular arrangement, even in controls (see Fig. 8). However, when Al-induced microfilament reorientation occurred, it was very obvious and, as observed for microtubules, random arrays of microfilaments were first detectable in the inner cortex. In contrast to microtubules, however, this observed effect occurred after the onset of growth inhibition and radial expansion (>6 h). Therefore, the reorientation of microfilaments could simply be a consequence of the changing polarity of the cells in the inner cortex. This is similar to cytoskeletal changes accompanying wound healing in roots, wherein microtubule reorganization has been shown to precede changes in the polarity of cells, whereas the reorganization of microfilaments occurs only after cells have already changed their growth direction (Hush and

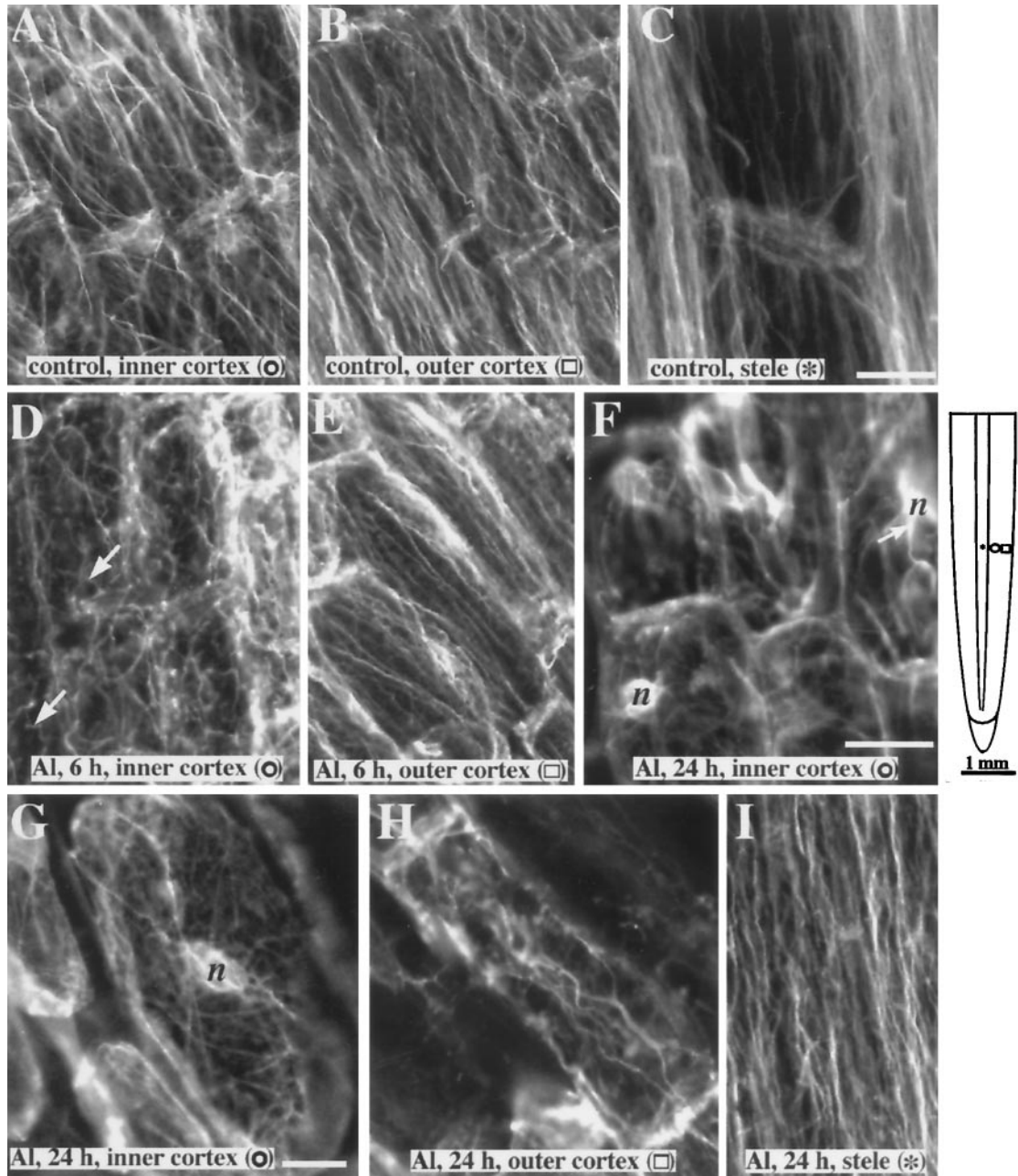
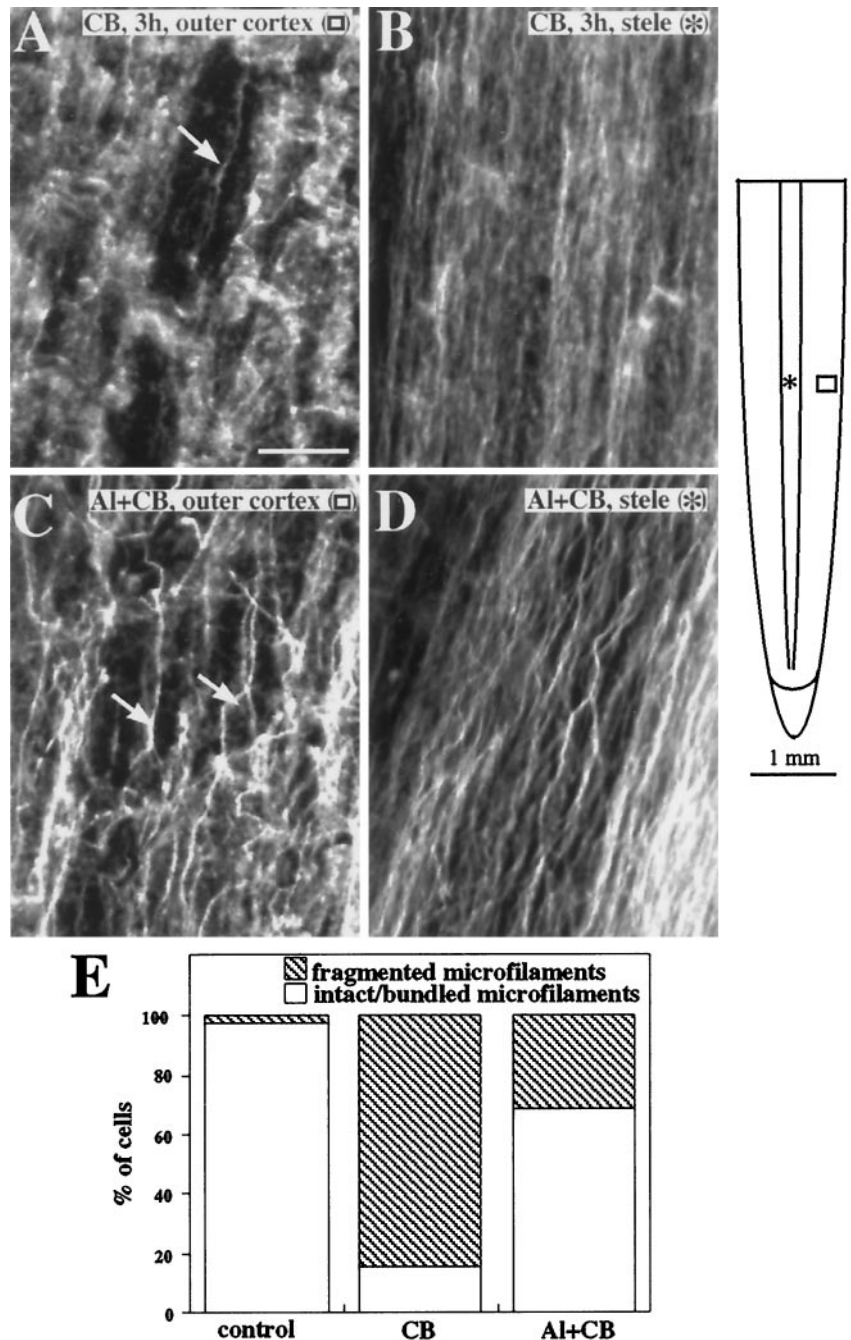


Figure 8. Organization of actin microfilaments in maize roots exposed to $50 \mu\text{M}$ Al. Microfilaments in the inner cortex (A), outer cortex (B) and stele (C) of control roots are parallel to the long axis of the cell. D, By 6 h of Al exposure, the inner cortical cells show a more random organization of microfilament bundles. Compared with the controls, microfilament bundles are not as straight (arrows). E, After 6 h the outer cortical cells still show a preferential longitudinal alignment of microfilaments. F, Microfilaments in the inner cortex after 12 to 24 h of Al exposure are randomly oriented. Thick microfilament bundles (arrow) appear to radiate from the nucleus (*n*). G, Higher-magnification image of an inner cortical cell after 24 h of Al exposure showing randomly oriented microfilaments. H, Outer cortical cells 24 h after Al treatment still show an overall longitudinal orientation of microfilaments, but microfilament bundles were generally thicker. I, Despite the disruption of microfilament organization in the other tissues, microfilaments in the stele were still longitudinal in orientation after a 24-h exposure to Al. The schematic diagram of the root indicates the regions where immunofluorescence images were obtained. Symbols in parentheses in A to I correspond to the symbols in the root diagram. Bar in C = $25 \mu\text{m}$ and applies to A to E and I; bar in F = $25 \mu\text{m}$ and applies to F and H; and bar in G = $10 \mu\text{m}$.

Figure 9. Organization of actin microfilaments in maize roots treated with the actin-depolymerizing agent CB (A and B) or Al plus CB (C and D). A, Microfilaments in the outer cortical cells of maize roots exposed to 50 μM CB for 3 h were completely disrupted. Only a few thick microfilament bundles remained (arrow). B, Microfilaments in the stele were also disrupted after CB treatment and characterized by thinner bundles. C, Cells in the outer cortex of roots pretreated with Al for 3 h still retained numerous thick microfilament bundles (arrows) even after exposure to CB. D, Microfilament bundles in the stele of Al-pretreated roots were thick and dense despite 3 h of exposure to CB. E, The fraction of cells in the outer cortex of CB-treated and Al-plus-CB-treated roots were classified by whether they had intact microfilaments or fragmented/no microfilaments. At least 50 cells were observed for each treatment. Images are representative of at least three roots from three independent experiments. The schematic diagram of the root indicates the regions where immunofluorescence images were obtained. Symbols in parentheses in A to D correspond to the symbols in the root diagram. Bar in A = 25 μm .



Overall, 1992). However, it is possible that the fixation protocol used in this study was not able to preserve the finer arrays of cortical microfilaments in the elongating cells. The microfilaments in the elongation zone observed in this study were primarily cytoplasmic bundles and changes in the finer arrays of microfilaments may have been missed.

The experiments described above with the microfilament antagonist CB also indicate that Al can induce a rapid (≤ 3 h) stabilization and bundling of the actin network, in agreement with results presented for soybean suspension cells (Grabski and Schindler, 1995; Grabski et al., 1998). This

observation is also supported by recent work showing that genes encoding fimbrin, a known actin-bundling protein in animals, are up-regulated in Al-treated wheat roots (Ortega et al., 1997). The stabilizing effect of Al on both the microtubules and microfilaments also indicates that both cytoskeletal components may respond to Al in a coordinated way, as has been reported previously in taxol-treated rye root tips (Chu et al., 1993).

Although these experiments indicate a significant interaction of Al with the root's cytoskeleton, the exact mechanisms involved remain unidentified. Because Al is known to rapidly enter cells (Lazof et al., 1994), it is possible that

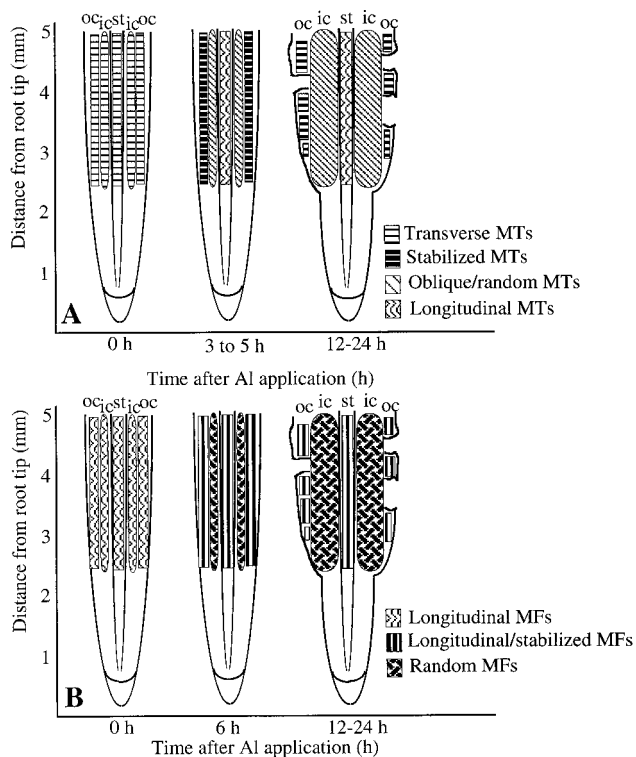


Figure 10. Schematic diagram of a longitudinal section of a maize root summarizing the changes in microtubules (MTs) (A) and microfilaments (MFs) (B) in the elongation zone after exposure to Al. A, Within 1 h of Al exposure, microtubules in the outer cortex (oc) were stabilized in the transverse orientation. Oblique to random microtubules were first detected in the inner cortex (ic) 3 h after Al exposure and after 4 h in the stele (st). This shift in microtubule orientation may lead to expansion of the inner cortical cells, resulting in root swelling. By 12 h, outer cortical cells with stabilized microtubules showed distorted shapes and were sloughed off from the root, leading to lesions along the root surface. B, Microfilaments were stabilized within 3 h after Al exposure. Randomly oriented and highly bundled microfilaments in the inner cortex and stele were detected 6 h after Al application. The stabilization and reorganization of microfilaments occurred later than that of microtubules.

it could interact directly with the cytoskeletal elements, as demonstrated *in vitro* by MacDonald et al. (1987). However, Al could also act indirectly through a modification of the cell's physiochemical environment, signal transduction pathways, or cytoskeletal anchors (Grabski et al., 1998). It is known that Al can interact strongly with the plasma membrane, resulting in disruptions in Ca^{2+} homeostasis, increased membrane rigidity, and a blockage of lipid-mediated signal transduction cascades (Deleers et al., 1986; Jones and Kochian, 1995, 1997). Because these are also known to be integrally involved in the regulation of plant cytoskeletal dynamics (Cyr, 1991; Xu et al., 1992; Shibaoka, 1994), it is likely that Al may act both directly and indirectly on the root's cytoskeleton.

ACKNOWLEDGMENTS

We thank Jo Hughes for performing the microtome sectioning and Richard Cyr for providing the anti-actin antibody. We also

thank Sian Ritchie and Richard Cyr for critical reading of the manuscript.

Received January 23, 1998; accepted May 31, 1998.

Copyright Clearance Center: 0032-0889/98/118/0159/14.

LITERATURE CITED

- Alfano F, Russel A, Gambardella R, Duckett JG (1993) The actin cytoskeleton of the liverwort *Riccia fluitans*: effects of cytochalasin B and aluminum on rhizoid tip growth. *J Plant Physiol* **142**: 569-574
- Andersland J, Fisher D, Wymer C, Cyr R, Parthasarathy M (1994) Characterization of a monoclonal antibody prepared against plant actin. *Cell Motil Cytoskel* **29**: 339-344
- Baluska F, Barlow PW, Volkmann D (1996) Complete disintegration of the microtubular cytoskeleton precedes its auxin-mediated reconstruction in postmitotic maize root cells. *Plant Cell Physiol* **37**: 1013-1021
- Baluska F, Brailsford RW, Hauskrecht M, Jackson MB, Barlow PW (1993a) Cellular dimorphism in the maize root cortex: involvement of microtubules, ethylene and gibberellin in the differentiation of cellular behavior in postmitotic growth zones. *Bot Acta* **106**: 394-403
- Baluska F, Parker JS, Barlow PW (1993b) The microtubular cytoskeleton in cells of cold-treated roots of maize (*Zea mays* L.) shows tissue-specific responses. *Protoplasma* **172**: 84-96
- Baluska F, Samaj J, Volkmann D, Barlow PW (1997) Impact of taxol-mediated stabilization of microtubules on nuclear morphology, ploidy levels and cell growth in maize roots. *Biol Cell* **89**: 221-231
- Baskin TI, Wilson JE (1997) Inhibitors of protein kinases and phosphatases alter root morphology and disorganize cortical microtubules. *Plant Physiol* **113**: 493-502
- Baskin TI, Wilson JE, Cork A, Williamson RE (1994) Morphology and microtubule organization in Arabidopsis roots exposed to oryzalin or taxol. *Plant Cell Physiol* **35**: 935-942
- Bennet RJ, Breen CM, Fey MV (1985) Aluminum induced changes in the morphology of the quiescent center, proximal meristem and growth region of the root of *Zea mays*. *S Afr J Bot* **51**: 355-362
- Blancaflor EB, Hasenstein KH (1993) Organization of cortical microtubules in graviresponding maize roots. *Planta* **191**: 231-237
- Blancaflor EB, Hasenstein KH (1995a) Effect of osmotic stress on growth and microtubule orientation of *Zea mays* roots. *Int J Plant Sci* **156**: 774-783
- Blancaflor EB, Hasenstein KH (1995b) Time course and auxin sensitivity of cortical microtubule reorientation in maize roots. *Protoplasma* **185**: 72-82
- Blancaflor EB, Hasenstein KH (1997) Organization of the actin cytoskeleton in vertical and graviresponding primary roots of maize. *Plant Physiol* **113**: 1447-1455
- Bokros CL, Hugdahl JD, Hanesworth VR, Murthy JV, Morejohn LC (1993) Characterization of the reversible taxol-induced polymerization of plant tubulin into microtubules. *Biochemistry* **32**: 3437-3447
- Chu B, Kerr GP, Carter JV (1993) Stabilizing microtubules with taxol increases microfilament stability during freezing of rye root tips. *Plant Cell Environ* **16**: 883-889
- Cyr RJ (1991) Calcium/calmodulin affects microtubule stability in lysed protoplasts. *J Cell Sci* **100**: 311-317
- Cyr RJ, Palevitz BA (1995) Organization of cortical microtubules in plant cells. *Curr Opin Cell Biol* **7**: 65-71
- Deleers M, Servais JP, Wulfert E (1986) Neurotoxic cations induce membrane rigidification and membrane fusion at micromolar concentrations. *Biochim Biophys Acta* **855**: 271-276
- Delhaize E, Craig S, Beaton CD, Bennet RJ, Jagadish VC, Randall PJ (1993) Aluminum tolerance in wheat (*Triticum aestivum* L.). I. Uptake and distribution of aluminum in root apices. *Plant Physiol* **103**: 685-693
- Drobak BK (1993) Plant phosphoinositides and intracellular signaling. *Plant Physiol* **102**: 705-709

- Fisher DD, Gilroy S, Cyr RJ** (1996) Evidence for opposing effects of calmodulin on cortical microtubules. *Plant Physiol* **112**: 1079–1087
- Giddings TH, Staehelin LA** (1991) Microtubule-mediated control of microfibril deposition: a re-examination of the hypothesis. *In* CW Lloyd, ed, *The Cytoskeletal Basis of Plant Growth and Form*. Academic Press, London, pp 85–99
- Grabski S, Arnoys E, Busch B, Schindler M** (1998) Regulation of actin tension in plant cells by kinases and phosphatases. *Plant Physiol* **116**: 279–290
- Grabski S, Schindler M** (1995) Aluminum induces rigor within the actin network of soybean cells. *Plant Physiol* **108**: 897–901
- Huang CN, Cornejo MJ, Bush DS, Jones RL** (1986) Improved methods for the determination of viability of plant protoplasts. *Protoplasma* **135**: 80–87
- Hush JM, Overall RL** (1992) Re-orientation of cortical F-actin is not necessary for wound-inducible microtubule re-orientation and cell polarity establishment. *Protoplasma* **169**: 97–106
- Jones DL, Kochian LV** (1995) Aluminum inhibition of the inositol 1,4,5-trisphosphate signal transduction pathway in wheat roots: a role in aluminum toxicity? *Plant Cell* **7**: 1913–1922
- Jones DL, Kochian LV** (1997) Aluminum interaction with plasma membrane lipids and enzyme metal binding sites and its potential role in Al cytotoxicity. *FEBS Lett* **400**: 51–57
- Jones DL, Kochian LV, Gilroy S** (1998) Aluminum induces a decrease in cytosolic $[Ca^{2+}]$ in BY-2 tobacco cell suspension cultures. *Plant Physiol* **116**: 81–89
- Kochian LV** (1995) Cellular mechanisms of aluminum toxicity and resistance in plants. *Annu Rev Plant Physiol Plant Mol Biol* **46**: 237–260
- Kochian LV, Jones DL** (1997) Aluminum toxicity and resistance in plants. *In* RA Yokel, MS Golub, eds, *Research Issues in Aluminum Toxicity*. Taylor and Francis, Washington, DC, pp 69–89
- Lazof DB, Goldsmith JG, Rufty TW, Linton RW** (1994) Rapid uptake of aluminum into cells of soybean root tips. *Plant Physiol* **106**: 1107–1114
- Le Van H, Kuraishi S, Sakurai N** (1994) Aluminum-induced rapid root inhibition and changes in cell-wall components of squash seedlings. *Plant Physiol* **106**: 971–976
- MacDonald TL, Humphreys WG, Martin RB** (1987) Promotion of tubulin assembly by aluminum ion in vitro. *Science* **236**: 183–186
- MacDonald TL, Martin RB** (1988) Aluminum ion in biological systems. *Trends Biochem Sci* **13**: 15–19
- Nixon RA, Clarke JF, Logvinenko KB, Tan MKH, Hoult M, Grynspan F** (1990) Aluminum inhibits calpain-mediated proteolysis and induces human neurofilament proteins to form protease resistant high molecular weight complexes. *J Neurochem* **55**: 1950–1959
- Ortega RC, Cushman JC, Ownby JD** (1997) cDNA clones encoding 1,3- β -glucanase and a fimbrin-like cytoskeletal protein are induced by Al toxicity in wheat roots. *Plant Physiol* **114**: 1453–1460
- Reid MS** (1995) Ethylene in plant growth, development, and senescence. *In* PJ Davies, ed, *Plant Hormones: Physiology, Biochemistry and Molecular Biology*. Kluwer Academic Publishers, Dordrecht, The Netherlands, pp 486–508
- Ryan PR, DiTomaso JM, Kochian LV** (1993) Aluminum toxicity in roots: an investigation of spatial sensitivity and the role of the root cap. *J Exp Bot* **44**: 437–446
- Sasaki M, Yamamoto Y, Matsumoto H** (1996) Lignin deposition induced by aluminum in wheat (*Triticum aestivum*) roots. *Physiol Plant* **96**: 193–198
- Sasaki M, Yamamoto Y, Matsumoto H** (1997) Aluminum inhibits growth and stability of cortical microtubules in wheat (*Triticum aestivum*) roots. *Soil Sci Plant Nutr* **43**: 469–472
- Schmidt R, Bohm K, Vater W, Unger E** (1991) Aluminum induced osteomalacia and encephalopathy: an aberration of the tubulin assembly into microtubules by Al^{3+} . *Prog Histochem Cytochem* **23**: 355–364
- Seagull RW** (1989) The plant cytoskeleton. *Crit Rev Plant Sci* **8**: 131–167
- Shea TB, Balikian P, Beermann ML** (1992) Aluminum inhibits neurofilament protein degradation by multiple cytoskeleton-associated proteases. *FEBS Lett* **307**: 195–198
- Shibaoka H** (1994) Plant hormone-induced changes in the orientation of cortical microtubules: alterations in the cross-linking between microtubules and the plasma-membrane. *Annu Rev Plant Physiol Plant Mol Biol* **45**: 527–544
- Siegel N, Haug A** (1983) Aluminum interaction with calmodulin: evidence for altered structure and function from optical and enzymatic studies. *Biochim Biophys Acta* **744**: 36–45
- Singer SM, Chambers CB, Newfry GA, Norlund MA, Muma NA** (1997) Tau in aluminum-induced neurofibrillary tangles. *Neurotoxicology* **18**: 63–76
- Sivaguru M, Horst WJ** (1998) The distal part of the transition zone is the most aluminum-sensitive apical root zone of maize. *Plant Physiol* **116**: 155–163
- Strong MJ, Garruto RM, Joshi JG, Mundy WR, Shafer TJ** (1997) Can the mechanisms of aluminum neurotoxicity be integrated into a single unified scheme? *In* RA Yokel, MS Golub, eds, *Research Issues in Aluminum Toxicity*. Taylor and Francis, Washington, DC, pp 207–239
- Taylor GJ** (1990) The physiology of aluminum phytotoxicity. *In* H Siegel, ed, *Metal Ions in Biological Systems*. Marcel Dekker, New York, pp 123–163
- Weerdenburg C, Seagull RW** (1988) The effects of taxol and colchicine on microtubule and microfibril arrays in elongating plant cells in culture. *Can J Bot* **66**: 1710–1716
- Xu P, Lloyd CW, Staiger CJ, Drobak BK** (1992) Association of phosphatidylinositol 4-kinase with the plant cytoskeleton. *Plant Cell* **4**: 941–951